BIOCHEMISTRY
including biophysical chemistry & molecular biology

New Concept

pubs.acs.org/biochemistry

The Crystal Structure of the C-Terminal Truncated Apolipoprotein A-I Sheds New Light on Amyloid Formation by the N-Terminal Fragment

Olga Gursky,* Xiaohu Mei, and David Atkinson

Department of Physiology and Biophysics, Boston University School of Medicine, Boston, Massachusetts 02118, United States

Supporting Information

ABSTRACT: Apolipoprotein A-I (apoA-I) is the main protein of plasma high-density lipoproteins (HDL, or good cholesterol) that remove excess cell cholesterol and protect against atherosclerosis. In hereditary amyloidosis, mutations in apoA-I promote its proteolysis and the deposition of the 9−11 kDa N-terminal fragments as fibrils in vital organs such as kidney, liver, and heart, causing organ damage. All known amyloidogenic mutations in human apoA-I are clustered in two residue segments, 26−107 and 154−178. The X-ray crystal structure of the C-terminal truncated human protein, Δ(185−243)apoA-I, determined to 2.2 Å resolution by Mei and Atkinson, provides the structural basis for understanding apoA-I destabilization in amyloidosis. The sites of amyloidogenic mutations correspond to key positions within the largely helical four-segment bundle comprised of residues 1−120 and 144−184. Mutations in these positions disrupt the bundle structure and destabilize lipid-free apoA-I, thereby promoting its proteolysis. Moreover, many mutations place a hydrophilic or Pro group in the middle of the hydrophobic lipid-binding face of the amphipathic α-helices, which will likely shift the population distribution from HDL-bound to lipid-poor/free apoA-I that is relatively unstable and labile to proteolysis. Notably, the crystal structure shows segment L44−S55 in an extended conformation consistent with the β-strand-like geometry. Exposure of this segment upon destabilization of the four-segment bundle probably initiates the α-helix to β-sheet conversion in amyloidosis. In summary, we propose that the amyloidogenic mutations promote apoA-I proteolysis by destabilizing the protein structure not only in the lipid-free but also in the HDL-bound form, with segment L44−S55 providing a likely template for the cross-β-sheet conformation.

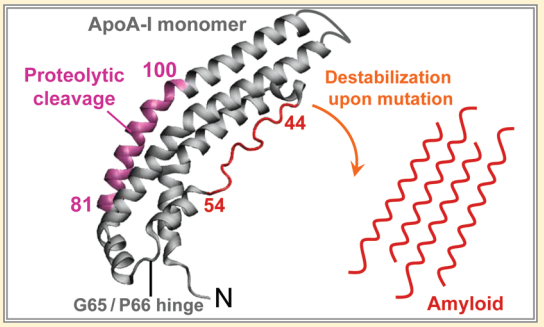

Plasma high-density lipoproteins (HDL) are heterogeneous nanoparticles comprised of 160−300 lipid molecules and two or more copies of water-soluble proteins termed exchangeable apolipoproteins. Amino acid sequences of these proteins contain 11/22-mer tandem repeats with a strong propensity to form amphipathic class A α-helices that are optimized for lipid surface binding.[1] The main HDL protein, apolipoprotein A-I (apoA-I, 243 amino acids), contains 10 such Pro-punctuated repeats (designated 1−10) encompassing residues 44−243, flanked by N-terminal segment 1−43 containing G* repeats.[2,3] Plasma levels of apoA-I and HDL correlate inversely with the incidence of atherosclerosis (refs 4−6 and references cited therein). This cardioprotective effect is mediated mainly via reverse cholesterol transport (RTC) whereby plasma HDL remove excess cholesterol from peripheral cells to the liver for excretion.[4−7]

More than 90% of circulating apoA-I is bound to HDL and is in dynamic equilibrium with the monomeric lipid-poor/free apoA-I that is generated either de novo or upon HDL remodeling in RCT.[6−9] This transient monomeric apoA-I is believed to be particularly cardioprotective because it provides the primary acceptor of cell cholesterol at the early rate-limiting step of RCT.[6,10] In contrast to HDL whose structure is stabilized by high kinetic barriers,[11] lipid-poor/free apoA-I adopts a molten globular conformation in solution[12] whose low thermodynamic stability facilitates its high metabolic activity.[13] Because lipid-poor/free apoA-I is more labile to proteolysis than its HDL-bound counterpart, a shift from HDL-bound to lipid-poor/free apoA-I is not necessarily beneficial.[14] In fact, enhanced proteolysis of lipid-poor/free apoA-I not only promotes protein degradation but also can lead to misfolding of the full-length protein or its proteolytic fragments and, eventually, protein deposition as amyloid fibrils.

OVERVIEW OF APOA-I AMYLOIDOSIS

ApoA-I is involved in two forms of amyloidosis. In non-hereditary form, full-length apoA-I is deposited in atherosclerotic plagues as fibrils whose clinical significance is just beginning to be elucidated.[15,16] In a hereditary form termed familial amyloidotic polyneuropathy (FAP), which is an autosomal dominant disorder, the N-terminal fragments of variant apoA-I are deposited as extracellular fibrils in organs such as kidney, liver, heart, spleen, skin, larynx, nerves, gastrointestinal tract, ovaries, and testes, leading to organ damage.[17−20] Currently, 19 FAP mutations in apoA-I (Table 1)

Received: November 11, 2011
Revised: December 12, 2011
Published: December 20, 2011

Table 1. Locations of the Amyloidogenic Mutations in the Crystal Structure of Δ(185−243)ApoA-I and Their Expected Structural Implications[a]

	mutation	sequence repeat	secondary structure	location in the bundle	expected effect on four-segment bundle packing
Mutations inside the N-Terminal Segment (1−100) That Can Form Fibrillar Deposits					
1	G26R	G*	helical kink	middle	disrupts L23−W50 cation−π interaction, destabilizes top hydrophobic cluster
2	E34K	G*	hinge	top	disrupts charge balance near the flexible hinge, which may alter the orientation of segment 1−34 in the four-segment bundle
3	W50R	1	extended strand	middle	replaces an attractive cation−π K23−W50 interaction with a repulsive K23−R50 interaction
4	L60R	1	α-helix	bottom	disrupts the bottom hydrophobic cluster
5	L64R	1	α-helix	bottom	disrupts the bottom hydrophobic cluster
6	L60−F71 deletion, V60 and T61 insertion	1 and 2	loop	bottom	deletes highly conserved G65, P66 hinge region that is critical for folding of the N-terminal bundle
7	E70−W72 deletion	2	α-helix	bottom	replaces an attractive cation−π K23−W50 interaction with a repulsive K23−R50 interaction
8	F71Y	2	α-helix	bottom	disrupts the bottom hydrophobic cluster by placing an OH group in it
9	N74K frame shift	2	α-helix	bottom	truncates the polypeptide chain, eliminates helical repeats 3−10
10	L75P	2	α-helix	bottom	disrupts the bottom hydrophobic cluster, possibly changes the relative helical orientation in the bundle
11	L90P	3	α-helix	middle	disrupts hydrophobic interactions, kinks the α-helix.
12	K107 deletion	4	α-helix	top	disrupts the salt bridge network involving K106, K107, E110, and E111 from repeat 4 and E147, R151, and H155 from repeat 6, alters α-helical orientation
Mutations outside the N-Terminal Segment (1−100)					
13	A154 frame shift	6	α-helix	top	truncates the protein in the middle of helical repeat 6 and eliminates the interactions between repeats 6, 7, and 2−4 such as the salt bridge network
14	H155M frame shift	6	α-helix	top	eliminates the salt bridge network involving sequence repeats 4 and 6, eliminates repeat 7
15	L170P	7	α-helix	bottom	kinks helical repeat 7, disrupts is interactions with helical repeat 2
16	R173P	7	α-helix	bottom	kinks helical repeat 7, disrupts is interactions with helical repeat 2
17	R174S	7	α-helix	bottom	places a polar group in the bottom hydrophobic cluster and disrupts it
18	A175P	7	α-helix	bottom	kinks helical repeat 7, disrupts is interactions with helical repeat 2
19	L178H	7	α-helix	bottom	places a polar group in the bottom hydrophobic cluster and disrupts it

[a]The location of each mutation site in the four-segment bundle observed in the crystal structure is indicated. The location of each mutation in the 11/22-mer sequence repeat of apoA-I is indicated by G or by numerals. The 11/22-mer residue sequence repeats in apoA-I are as follows: G* repeats (residues 1−43), repeat 1 (residues 44−65), repeats 2 and 3 (residues 66−98), repeat 4 (residues 99−120), repeat 5 (residues 121−142), repeat 6 (residues 143−164), repeat 7 (residues 165−185), repeat 8 (residues 186−208), repeat 9 (residues 209−219), and repeat 10 (residues 220−241).

dx.doi.org/10.1021/bi2017014 | Biochemistry 2012, 51, 10−18

that promote apoA-I processing by metalloproteases and release of the N-terminal 9−11 kDa fragments that deposit as amyloid have been identified.[20] The fibrillar deposits in the heart contain mainly fragment 1−93, while those in other organs contain slightly shorter or longer fragments ranging from approximately 1−80 to 1−100.[18]

The broad clinical presentation of the disease associated with the same apoA-I mutation can vary from severe (renal failure at a young age) to moderate symptoms, suggesting that factors other than the mutation per se affect amyloidosis.[20] The lipid environment is one factor that has been proposed to have an important effect on fibril formation by apoA-I and other amyloidogenic proteins.[21,22] The role of HDL lipid composition in apoA-I amyloidosis is unclear and will be discussed below.

A common symptom of FAP is renal impairment that apparently results from increased catabolism of apoA-I rather than its overproduction. In contrast to other systemic amyloidoses involving protein overproduction, FAP patients have lower than normal (30−50%) plasma levels of apoA-I and HDL,[17,18] which results from decreased levels of secretion of the mutant protein and/or its increased catabolism.[23,24] Interestingly, despite low levels of apoA-I and HDL, FAP patients do not show an increase in coronary artery disease,[17,18] suggesting that low levels of HDL are offset by more efficient reverse cholesterol transport in these patients. The deposition of apoA-I in FAP is proposed to result from the structural destabilization of apoA-I by mutations and the ensuing proteolysis that generates a critical concentration of the partially folded amyloid precursor.[18] The nature of this precursor is unclear and will be addressed in this work.

The first and most common amyloidogenic mutation found in apoA-I is the Iowa variant, G26R.[17,23] This and other amyloidogenic mutations that have been identified in the N-terminal half of apoA-I led to a notion that FAP involves destabilization of the N-terminal region of apoA-I.[17] Later, additional amyloidogenic mutations have been found inside and outside the N-terminal region (Table 1). Mass spectroscopic analysis of several variants containing mutations either inside (E34K and F75Y) or outside the N-terminal half of apoA-I (H155M frame shift and A175P) revealed that only the fragments of the mutant protein are deposited as fibrils,[20] whereas earlier studies of other "outside" mutants such as L187H reported that amyloid deposits contained both full-length apoA-I and its N-terminal fragments.[25] Notably, for the "outside" mutations, the N-terminal protein fragments found in fibrillar deposits are mutation-free. Consequently, these mutations promote apoA-I proteolysis by destabilizing the overall protein conformation that includes (but is not limited to) its N-terminal region, rather than by increasing the aggregation rate of the N-terminal fragment.[18,26] In addition, some but not all "inside" mutations can enhance the rate of fibril formation by the N-terminal fragment in vitro.[27] Currently, there are 19 known amyloidogenic mutations in apoA-I which form two "hot spots": residues 26−107 from repeats G* and 1−4 in the N-terminal half of apoA-I and residues 154−178 from repeats 6 and 7 in the C-terminal half (Table 1). The implications of these mutations for the structure and stability of apoA-I in the lipid-free state in solution and in the lipid-bound state on HDL are unclear and are the focus of this work.

Several lines of evidence suggest that self-association of apoA-I in solution and amyloid formation proceed via distinctly different pathways. First, all amyloid deposits in FAP contain the N-terminal segment, whereas the primary self-association and lipid binding site in the full-length apoA-I encompasses its most hydrophobic C-terminal segment, 190−243 (ref 28 and references cited therein). Second, in vitro studies of recombinant apoA-I fragment 1−93 containing various amyloidogenic mutations did not show a clear correlation between the rate of protein aggregation and its propensity to form amyloid.[27] Furthermore, the metabolic fate of the N-terminal fragment depends critically upon its length: shorter fragments such as the 9−11 kDa polypeptides found in FAP are deposited as fibrils, whereas longer fragments such as the ∼18 kDa polypeptide released in the nonamyloidogenic apoA-I Fin variant, L159R, follow the degradative rather than amyloidogenic pathway.[29,30] The structural basis for this difference is unclear and will be discussed below.

The high-resolution structure of apoA-I is the necessary basis for understanding the protein function in the healthy state and in pathologic conditions such as amyloidosis. For nearly three decades, the high-resolution structure of apoA-I has eluded determination because of the conformational plasticity of this protein and its propensity to self-associate. This problem was overcome by Mei and Atkinson who crystallized the recombinant human C-terminal deletion mutant, Δ(185−243)apoA-I, and determined its X-ray crystal structure to 2.2 Å resolution.[31] Because this deletion mutant contains all sites of known amyloidogenic mutations in apoA-I, it provides an excellent model for understanding the structural implications of these mutations. Mapping the sites of amyloidogenic mutation on the high-resolution crystal structure of Δ(185−243)apoA-I allows us to gain novel insights into the likely effects of these mutations on the structure and stability of lipid-free and lipid-bound apoA-I and to propose a possible pathway of amyloid formation by variant human apoA-I.

OVERVIEW OF THE X-RAY CRYSTAL STRUCTURE OF Δ(185−243)APOA-I

In the crystal structure, lipid-free Δ(185−243)apoA-I forms a dimer comprised of two antiparallel molecules adopting an ∼80% α-helical semicircular conformation with a diameter d ≈11 nm that is comparable to the HDL diameter (Figure 1A). The sequence repeat registry observed in the two dimer-forming molecules, with the juxtaposed copies of central repeat 5 (Figure 1), is similar to that reported in the low-resolution crystal structure of the N-terminal truncation mutant, Δ(1−43)apoA-I,[32] and in the cross-linking studies of apoA-I on model and plasma HDL (refs 4 and 5 and references cited therein). This similarity, together with the demonstrated ability of Δ(185−243)apoA-I to form functional HDL-like complexes with model phospholipids and cholesterol, indicates that this crystal structure depicts key aspects of the functional apoA-I conformation in the lipid-free form as well as on HDL.[31,33]

The overall molecular curvature of the Δ(185−243)apoA-I dimer is induced by the Pro-containing helical kinks that are in registry in the two antiparallel dimer-forming molecules. The structure is stabilized by two symmetry-related four-segment bundles at the opposite ends of the dimer (Figure 1A). Each bundle is comprised of three segments formed by residues 1−120 (sequence repeats G* and 1−4) from one molecule (Figure 1B) and the fourth segment formed by residues 143−184 (sequence repeats 6 and 7) from the second molecule within the dimer. The bundle is largely α-helical, except for segment L44−S55 (containing 11-mer sequence repeat 44−54)

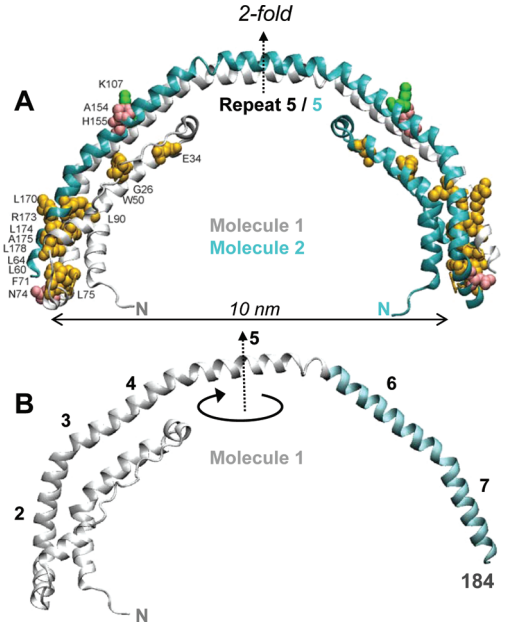

Figure 1. Locations of amyloidogenic mutations in the structure of apoA-I. (A) X-ray crystal structure of Δ(185−243)apoA-I (Protein Data Bank entry 3R2P[31]) showing a crystallographic dimer comprised of molecule 1 (gray) and molecule 2 (teal). The crystallographic 2-fold axis that passes through the middle of sequence repeat 5 (residues 121−142) is indicated. Residues in the nonvariant apoA-I that are mutated in hereditary amyloidosis are shown in space-filling representation and are color-coded: yellow for point substitutions, green for deletions, and pink for frame shift mutations. The figure was obtained by using Swiss Protein Data Bank and VMD molecular graphics. (B) Molecule 1 from the crystallographic dimer of Δ(185−243)apoA-I, in which 11/22-mer residue sequence repeats G* and 1−7 are indicated. Repeats 8−10 encompassing residues 186−243 have been truncated from Δ(185−243)apoA-I. Helical repeats 6 and 7 are colored teal; upon conversion of the apoA-I dimer to the monomer, these repeats are proposed to undergo domain swapping by folding back around the dimer 2-fold axis that passes through the middle of repeat 5 (circular arrow).

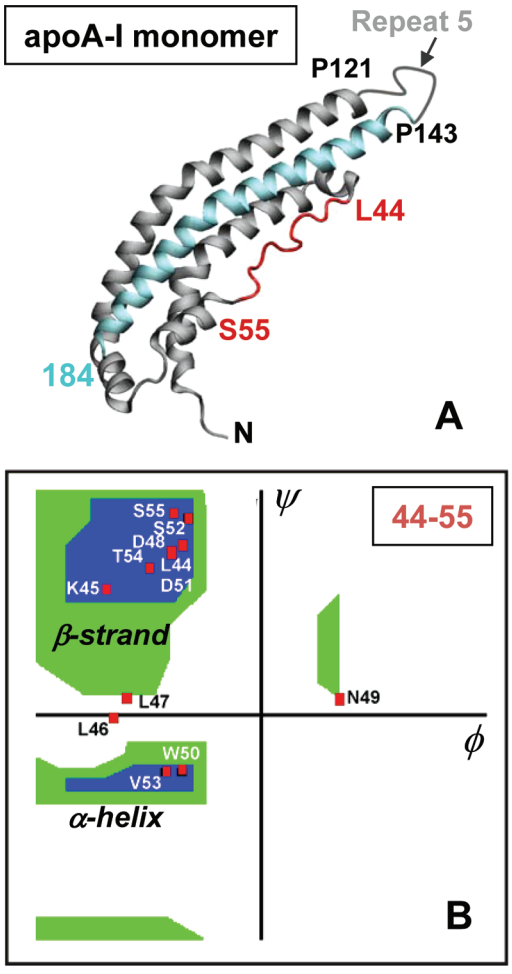

Figure 2. Structure inferred for the lipid-free C-terminal truncated apoA-I monomer and the conformation of the extended segment, L44−S55. (A) The monomer structure was obtained by using molecule 1 of the dimer structure (Figure 1) that is folded back around the middle of central repeat 5 (residues 121−142). Such folding represents domain swapping of helical sequence repeats 6 and 7 (residues 143−185, teal) from molecule 2 to molecule 1. Extended segment L44-S55 is colored red. (B) Ramachandran plot for the peptide groups from extended segment L44−S55 showing that the torsion angles observed in most of these groups are consistent with the *β*-strand conformation.

that forms an extended structure (Figure 2, red). Each four-segment bundle is stabilized by a cation−*π* interaction between K23 and W50 located in the middle of the extended structure, and by two hydrophobic clusters, one at the top and another at the bottom of the bundle.[31] The "top" cluster contains aromatic (F33, F104, and W108) and aliphatic (V30, L38, L42, L44, and L46) residues from molecule 1, along with V156 and L159 from molecule 2. The "bottom" cluster is more extensive and contains closely packed aromatic (F71, W72, and W8 that forms a cation−*π* interaction with R61) and aliphatic (L14, L60, L64, and L75) groups from molecule 1 forming a leucine zipper with L170, L174, L178, and L181 from molecule 2.

How does the crystal structure of the lipid-free Δ(185−243)apoA-I dimer relate to that of the lipid-free apoA-I monomer in solution? In monomolecular lipid-free apoA-I, the polypeptide chain is proposed to fold back upon itself near the middle of central repeat 5 (residues 121−143) (Figure 1B, circular arrow), leading to domain swapping of helical segment 143−184 (repeats 6 and 7), from the bundle in molecule 2 to a similar bundle in molecule 1.[31] Hence, the lipid-free apoA-I monomer is proposed to form a four-segment bundle similar to that observed in the crystallographic dimer, but with all four segments belonging to the same molecule (Figure 2A). Furthermore, in the full-length apoA-I monomer in solution, hydrophobic C-terminal segment 185−243 (repeats 8−10) is suggested to be largely disordered in the lipid-free state (refs 31 and 33 and references cited therein). Hence, the conformation of Δ(185−243)apoA-I in the truncated protein is representative of that in full-length apoA-I.

In summary, the crystal structure of dimeric lipid-poor Δ(185−243)apoA-I provides an extremely useful model for understanding the molecular packing of apoA-I in the monomeric lipid-poor/free state and on HDL. The information obtained from this model is key to understanding the structural consequences of specific mutations in lipid-free and HDL-bound apoA-I.

■ AMYLOIDOGENIC MUTATIONS DESTABILIZE THE FOUR-SEGMENT BUNDLE IN LIPID-FREE APOA-I

All 19 known amyloidogenic mutations in apoA-I are clustered in two hot spots encompassing residues 26−107 and 154−178.

dx.doi.org/10.1021/bi2017014 | *Biochemistry* 2012, 51, 10−18

Mapping these mutations on the crystal structure of Δ(185−243)apoA-I reveals that these hot spots are packed against each other in the four-segment bundle (Figure 1A). This suggests strongly that the perturbations of this bundle structure induced by mutations are key to hereditary apoA-I amyloidosis. As summarized in Table 1, analysis of individual mutation sites suggests a molecular mechanism via which each amyloidogenic mutation destabilizes the molecular packing in lipid-free and HDL-bound apoA-I, thereby promoting dissociation of apoA-I from HDL followed by proteolysis and misfolding of the N-terminal fragment. Below, we describe the locations of four representative amyloidogenic mutations in the crystal structure, including the two most common mutations (G26R and L75P), one conservative mutation (F71Y), and one "outside" mutation (L75P). Locations of the 15 additional mutations and their expected structural implications are described in the Supporting Information.

G26R Substitution. The site of this most common amyloidogenic mutation, termed apoA-I Iowa,[23] is depicted in Figure 3A. In the crystal structure, G26 forms a kink in the middle of the first helical segment of the four-segment bundle, conferring the curvature to this segment which complements the overall molecular curvature of apoA-I and HDL. The G26R substitution is expected to reduce the flexibility of the polypeptide chain and alter the curvature of this segment. Moreover, the G26R substitution places a positive charge next to K23, which replaces the attractive cation−π interaction between K23 and W50 with a repulsive interaction between K23 and R26 and thereby destabilizes extended region L44−S55 in which residue 50 is located (Figure 2, red). As described below, increased solvent exposure of this extended region is likely to promote amyloid formation.

F71Y Substitution. The site of this most conservative amyloidogenic mutation is depicted in Figure 3B. F71 is located in the bottom aromatic cluster in a highly hydrophobic environment created by W8, W72, F71, L14, L60, L64, L75, L170, L174, L178, and L181. The F71 phenol ring is nearly orthogonal to and forms stacking interactions with the indole rings of W8 and W72. The F71Y substitution places an OH group in this tightly packed hydrophobic cluster, thereby destabilizing it. If, as a result of this substitution, the Y71 side chain flips out into a more polar environment, the bottom aromatic cluster is disrupted.

L75P Substitution. The location of this common amyloidogenic mutation[34] is depicted in Figure 3C. L75 is located in the middle of short helix 70−76 that defines, in part, the relative helical orientation in the four-segment bundle. Also, L75 interacts with L14 in the bottom hydrophobic cluster. The L75P substitution not only disrupts this interaction but also imposes constraints on the relative orientation of the bundle-forming helices, which is expected to destabilize the four-segment bundle.

R173P Substitution. The location of this outside mutation is depicted in Figure 3D. The R173P substitution induces a kink in helical sequence repeat 7 (residues P165−G185). This is expected to disrupt the interactions of this helical segment with the juxtaposed helical segment from repeats 2 and 3 at the bottom of the bundle and thereby disrupt the bottom hydrophobic cluster.

In summary, the crystal structure of Δ(185−243)apoA-I suggests strongly that all known amyloidogenic mutations destabilize the four-segment bundle in the lipid-free protein. Furthermore, the amyloidogenic mutations fall into several major groups according to their location and the expected destabilizing effect on the bundle structure (Table 1). Eleven mutations (L60R, L64R, L60−F71 deletion/V60 and T61 insertion, F70−W72 deletion, F71Y, L75P, L170P, R173P, L174S, A175P, and L178H) disrupt the packing at the bottom of the four-segment bundle; three mutations (G26R, W50R, and L90P) disrupt the packing in the middle of the bundle, and two mutations (E34K and K107 deletion) disrupt the top of the bundle. The three remaining mutations involve frame shifts in juxtaposed helical repeats 4 and 6 leading to a premature termination of the polypeptide chain, which eliminates one or more segments from the four-segment bundle. Hence, destabilization of the four-segment bundle in lipid-free apoA-I is an apparent unifying property of all known amyloidogenic mutations.

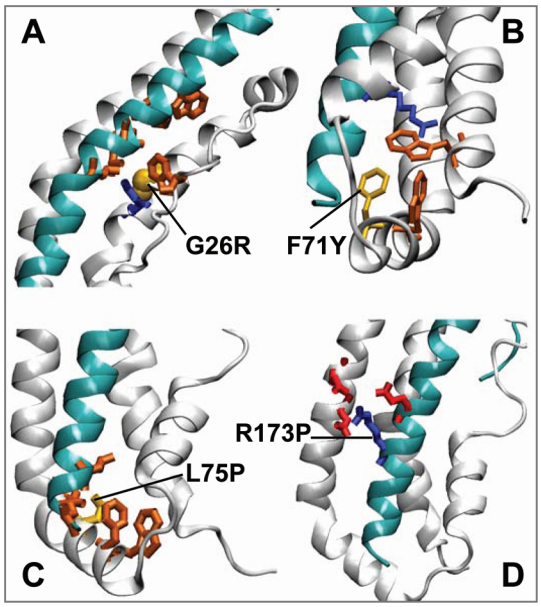

Figure 3. Residue packing at the sites of selected amyloidogenic mutations. The packing in the crystal structure of Δ(185−243)apoA-I is shown. Sequence repeats G* and 1−4 are colored gray, and repeats 6 and 7 are colored teal. The four selected mutations are indicated in the panels. The residues in the crystal structure of apoA-I that are subjected to mutations are shown, together with their nearest neighbors. Hydrophobic groups are colored yellow (variant residue) or orange (its nearest neighbors), acidic groups red, and basic groups blue, and Gly is shown in space-filling representation.

PATHOLOGIC IMPLICATIONS OF THE DESTABILIZATION OF THE FOUR-SEGMENT BUNDLE

Why do the mutations listed in Table 1 lead to proteolytic cleavage at sites between residues 80 and 100 in sequence repeats 3 and 4? Even though the details of the apoA-I proteolysis at these sites are not well-understood, it is clear that increased solvent exposure of sequence repeats 3 and 4 in apoA-I, along with the structural disordering of these repeats, facilitates their proteolytic cleavage. In the crystal structure, helical repeats 2−4 (residues 77−121) are paired with the juxtaposed helical repeats 6 and 7 (residues 143−184) in the four-segment bundle (Figures 1 and 4). Disruption of the extensive packing interactions between repeats 2−4 and repeats 6 and 7 as a result of mutations in these repeats is expected to increase the solvent exposure of repeats 2−4. Furthermore,

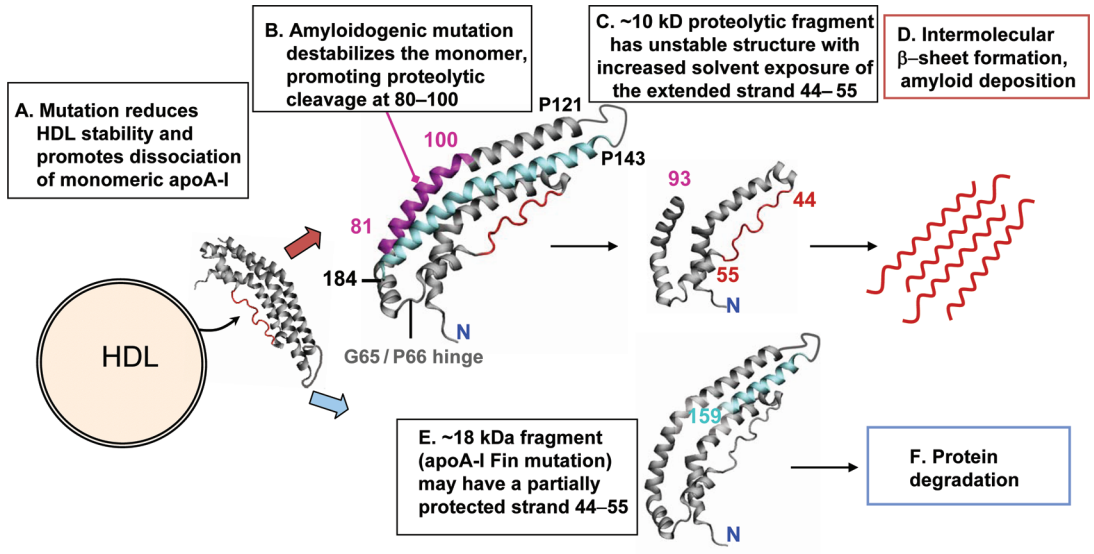

Figure 4. Proposed pathways for processing of apoA-I mutants in amyloidosis and degradation. The red arrow indicates the amyloidogenic pathway and the blue arrow the degradative pathway. (A) Mutation of apoA-I reduces the affinity of protein for lipid and thereby shifts the population distribution, from HDL-bound to lipid-poor/free monomeric apoA-I. (B) In the amyloidogenic pathway, the four-segment bundle in the apoA-I monomer in solution is destabilized by the mutation that disrupts the packing interactions involving repeats 2−4 (including residues 81−120, purple), rendering them labile to proteolysis. (C) The resulting ~10 kDa proteolytic fragment is missing approximately one and one-half helical segments from the four-segment bundle and is unfolded in solution.[27] This increases the solvent exposure of the extended segment of L44−S55 (red) that is primed for β-sheet formation. (D) L44−S55 segments initiate the intermolecular cross-β-sheet conformation in amyloid. (E) In the degradative pathway, the relatively large proteolytic fragment (~18 kDa) has a largely intact four-segment bundle. This renders some protection to the extended segment L44−S55 and thereby hampers intermolecular β-sheet formation.

mutations elsewhere in the structure that destabilize the four-segment bundle can lead to bundle opening by rotation around the hinge region centered at G65 and P66 (Figure 4). Such a hinge motion will increase the solvent exposure of repeats 2−4, rendering them labile to proteolysis.

Why are N-terminal fragments 1−80 to 1−100 amyloidogenic whereas longer fragments, such as the ~18 kDa N-terminal fragment in the apoA-I Fin variant, do not form amyloid?[29,30] We speculate that in the longer fragments such as the apoA-I Fin, the four-segment bundle is largely intact and, hence, the L44−S55 segment is substantially protected from the solvent (Figure 4E). In contrast, shorter ~10 kDa fragments are missing one or more helical segments from the four-segment bundle (Figure 4C), rendering them unfolded in solution.[27] This leads to increased solvent exposure of the extended segment L44−S55 that, as proposed below, likely initiates the β-sheet conformation in amyloid.

EXTENDED SEGMENT L44−S55 PROBABLY NUCLEATES THE AMYLOID β-SHEET

The crystal structure of Δ(185−243)apoA-I shows an ~80% α-helical conformation with only two extended nonhelical segments, one encompassing residues 1−8 from the Pro-rich N-terminal region[35] and another encompassing residues 44−55 containing the 11-mer sequence repeat 1 that forms the sole nonhelical region in the four-segment bundle (Figure 3A). This observation is consistent with the earlier studies showing that residues 44−55 have the lowest degree of sequence homology with the rest of the 11/22-mer sequence repeats in apoA-I.[2,31] Importantly, the Ramachandran plot based on the crystal structure of Δ(185−243)apoA-I shows that most residues in extended region L44−S55, including L44, K45, D48, D51, S52, T54, and S55, have main chain torsion angles (ϕ and ψ) in the β-strand range (Figure 3B). This is in stark contrast with the rest of the crystal structure showing that the groups whose torsion angles are consistent with the β-structure are sparse, singular, and limited to interhelical kinks, loops, or Pro-rich N-terminal residue segment 1−8. Interestingly, a short N-terminal β-strand spanning residues 20−25 was inferred from the EPR studies by Oda and colleagues and was proposed to extend beyond G26 in apoA-I Iowa variant G26R (ref 36 and references cited therein). The discrepancy in the location of the N-terminal β-strand inferred by EPR studies and observed in the crystal structure of Δ(185−243)apoA-I is unclear. This discrepancy is unlikely to result from the deletion of C-terminal segment 185−243, because in the lipid-free protein this segment is largely disordered and does not form substantial interactions with the N-terminal bundle (refs 31, 33, and 37 and references cited therein). Alternatively, the discrepancy can result from the environmental effects on the local protein conformation, including the effects of the spin-labels used in EPR experiments, as well as the effects of lipids. Interestingly, in the recent EPR study of apoA-I on model HDL by the same group of authors, an unstructured segment was inferred for residues 35−39 and a β-strand for residues 40−49,[38] which is in better agreement with the crystal structure. This agreement is consistent with the notion that the crystal structure represents an intermediate between the lipid-free and lipid-bound protein conformations.[31]

In summary, the crystal structure of Δ(185−243)apoA-I allows the first direct observation of the extended conformation in residue segment 44−55 that is consistent with the β-strand-like geometry. This observation suggests a unique structural role for segment 44−55 in the highly α-helical protein. In the crystal structure, the extended nonhelical conformation of this segment is dictated by its packing against the longer 18-residue helical segment 20−37, and the opening provided by their packing is proposed to provide an entry point for lipids.[31] We

dx.doi.org/10.1021/bi2017014 | *Biochemistry* 2012, 51, 10−18

posit that segment 44−55 can provide a template for the formation of an intermolecular β-sheet. Therefore, destabilization of the four-segment bundle by mutations, proteolysis, or other perturbations that increase the solvent exposure of extended segment L44−S55 is expected to promote amyloid nucleation.

AMYLOIDOGENIC MUTATIONS CAN DESTABILIZE LIPID-FREE AND HDL-BOUND APOA-I

The X-ray crystal structure of Δ(185−243)apoA-I demonstrates, for the first time, that the sites of all known amyloidogenic mutations in apoA-I are located in the four-segment bundle that confers structural stability to the lipid-poor/free protein. The crystal structure suggests strongly that all known amyloidogenic mutations (and, possibly, others that are still unknown) destabilize the four-segment bundle, leading to solvent exposure of helical repeats 3 and 4 (residues 81−120) and the ensuing proteolysis in this region. Destabilization of the four-segment bundle by mutations helps explain the enhanced catabolism of the variant protein versus normal apoA-I observed in heterozygous carriers.[17,18,23] Furthermore, apoA-I cleavage at sites between residues 80 and 100 releases relatively short N-terminal proteolytic fragments that lack approximately one and one-half to two helical segments from the four-segment bundle (Figure 4C). This destabilizes the bundle structure, leading to its unfolding[27] and increased solvent exposure of extended segment L44−S55. The geometry of this segment observed in the crystal structure suggests strongly that it has a high intrinsic propensity to form a β-sheet (Figure 2) and, hence, provides a likely template for the cross-β-sheet conformation in amyloid.

Are the pathologic effects of the amyloidogenic mutations limited to the structural destabilization of the lipid-free protein, or do they also involve destabilization of apoA-I on HDL? Although a definitive answer awaits experimental determination by measurement of the structural stability of model HDL containing variant forms of apoA-I, we speculate that many amyloidogenic mutations reduce the affinity of apoA-I for the phospholipid surface and thereby destabilize HDL. Such mutations include point substitutions that place Pro (L75P, L90P, L170P, R173P, and A175P), charged (G26R, W50R, L60R, and L64R) or polar (L174S and L178H) residues in the apolar lipid-binding face of an amphipathic α-helix, thereby reducing protein affinity for lipid (Table 1). The effects of these substitutions are reminiscent of modifications in Met residues that are located on the apolar faces of the amphipathic α-helices in apoA-I: Met modifications such as oxidation, which place a hydrophilic group in the middle of the hydrophobic helical face, reduce protein stability in the lipid-free and HDL-bound states, increase the susceptibility of apoA-I to proteolysis, and promote amyloid formation by full-length apoA-I.[39−42] Similar effects are expected to drive amyloid formation by many point substitution mutants of apoA-I that place a hydrophilic group in the hydrophobic helical face.

Other amyloidogenic mutations in apoA-I involve truncations of large amphipathic helical segments upon frame shifts, including N74K frame shift, A154 frame shift, and H155M frame shift (Table 1). These truncations eliminate large lipid-binding surfaces (including C-terminal helical repeats 8−10 that form the primary lipid binding site in apoA-I) and thereby reduce the affinity of protein for lipid. Furthermore, point deletions such as L60−F71 deletion/V60 and T61 insertion, E70−W72 deletion, or K107 deletion (Table 1) are expected to change the helical orientation and/or partially unfold the helices, which is expected to destabilize HDL. In fact, deletion of L107 was demonstrated to reduce the structural stability of apoA-I in solution and on model HDL,[40] which supports our hypothesis.

HDL destabilization by amyloidogenic mutations (Table 1) is expected to promote dissociation of apoA-I from the HDL surface, leading to formation of the monomeric lipid-poor/free apoA-I that is more labile to proteolysis than its HDL-bound counterpart. Even in the absence of proteolysis, dissociation of highly helical apolipoproteins from HDL and formation of partially folded intermediates are thought to be prerequisites for amyloid formation.[43] Consequently, HDL stability is expected to be an important determinant for amyloid formation. This prompts us to speculate that, in addition to apoA-I mutations, other factors that destabilize HDL assembly, such as the increased free fatty acid content on the HDL surface[44] or the increased triacylglycerol content in the HDL core,[45] may promote apoA-I amyloidosis. The effects of these factors on amyloid formation by apoA-I will be explored in future studies.

SUMMARY AND FUTURE STUDIES

We propose that amyloidogenic mutations in apoA-I can contribute to fibril formation via several mechanisms. First, they destabilize HDL and promote apoA-I dissociation in the lipid-poor/free form that is relatively unstable and labile to proteolysis. Second, they destabilize the four-segment bundle in the lipid-poor/free apoA-I, which leads to partial unfolding and increased solvent exposure of residue segment 80−100, thereby increasing the susceptibility of this segment to cleavage by metalloproteases. Third, they increase the solvent exposure of extended segment L44−S55 that has high β-sheet propensity and likely forms a template for the cross-β-sheet conformation in amyloid.

One way to experimentally test these hypotheses in the future is to compare the stability of the recombinant mutant full-length apoA-I in solution and on HDL with that of the wild-type protein. Second, once the proteases involved in the apoA-I cleavage at positions 80−100 have been identified, they can be used to test for increased susceptibility of the amyloidogenic versus nonamyloidogenic protein variants to proteolysis at these positions. Third, the structure and stability of ∼18 kDa fragments of apoA-I such as 1−159 (apoA-I Fin) that do not form amyloid in vivo can be tested in solution and on HDL, and their propensity to misfold under amyloid-promoting conditions in vitro can be compared with that of the amyloidogenic ∼10 kDa fragments such as 1−93. Fourth, the position of the repeat 1-containing extended segment 44−55 and juxtaposed repeats 2 and 3 in the four-segment bundle can be locked by using structure-based engineered disulfides, to test if such "locking" prevents amyloid formation in vitro. Fifth, recombinant apoA-I in which sequence repeat 1 has been replaced with a more canonical class A helical repeat can be analyzed to test if such a replacement impairs amyloid formation. Finally, synthetic peptide fragments of nonvariant apoA-I, particularly those encompassing segment 44−55, can be used to test their ability to form the cross-β-sheet conformation.

ASSOCIATED CONTENT

Supporting Information

In addition to four mutation sites shown in Figure 3 (G26, F71Y, L75P, and R173P), locations of 15 naturally occurring

dx.doi.org/10.1021/bi2017014 | Biochemistry 2012, 51, 10−18

human amyloidogenic mutations in the crystal structure of the C-terminal truncated apoA-I, including mutations E34K, W50R, L60R, L64R, L60−F71 deletion/V60 and T61 insertion, E70−W72 deletion, N74K frame shift, L90P, K107 deletion, A154 frame shift, H155M frame shift, L170P, L174S, A175P, and L178H. This material is available free of charge via the Internet at http://pubs.acs.org.

AUTHOR INFORMATION

Corresponding Author

*Department of Physiology and Biophysics, W329, Boston University School of Medicine, 700 Albany St., Boston, MA 02118. E-mail: gursky@bu.edu. Phone: (617) 638-7894. Fax: (617) 638-4041.

Funding

This work was supported by National Institutes of Health Grants P01 HL026335 and RO1 GM067260.

ACKNOWLEDGMENTS

We are indebted to Dr. Shobini Jayaraman for extremely useful discussions and help throughout this work.

ABBREVIATIONS

HDL, high-density lipoproteins; apo, apolipoprotein; RCT, reverse cholesterol transport; FAP, familial amyloid polyneuropathy or hereditary apoA-I amyloidosis.

REFERENCES

(1) Segrest, J. P., Jones, M. K., De Loof, H., Brouillette, C. G., Venkatachalapathi, Y. V., and Anantharamaiah, G. M. (1992) The amphipathic helix in the exchangeable apolipoproteins: A review of secondary structure and function. *J. Lipid Res. 33* (2), 141−166.

(2) Nolte, R. T., and Atkinson, D. (1992) Conformational analysis of apolipoprotein A-I and E-3 based on primary sequence and circular dichroism. *Biophys. J. 63* (5), 1221−1239.

(3) Bashtovyy, D., Jones, M. K., Anantharamaiah, G. M., and Segrest, J. P. (2011) Sequence conservation of apolipoprotein A-I affords novel insights into HDL structure-function. *J. Lipid Res. 52* (3), 435−450.

(4) Lund-Katz, S., and Phillips, M. C. (2010) High density lipoprotein structure-function and role in reverse cholesterol transport. *Subcell. Biochem. 51*, 183−227.

(5) Huang, R., Silva, R. A., Jerome, W. G., Kontush, A., Chapman, M. J., Curtiss, L. K., Hodges, T. J., and Davidson, W. S. (2011) Apolipoprotein A-I structural organization in high-density lipoproteins isolated from human plasma. *Nat. Struct. Mol. Biol. 18* (4), 416−422.

(6) Yvan-Charvet, L., Wang, N., and Tall, A. R. (2010) Role of HDL, ABCA1, and ABCG1 transporters in cholesterol efflux and immune responses. *Arterioscler. Thromb. Vasc. Biol. 30*, 139−143.

(7) Fielding, C. J., and Fielding, P. E. (1995) Molecular physiology of reverse cholesterol transport. *J. Lipid Res. 36*, 211−228.

(8) Rye, K. A., Clay, M. A., and Barter, P. J. (1999) Remodelling of high density lipoproteins by plasma factors. *Atherosclerosis 145*, 227−238.

(9) Cavigiolio, G., Geier, E. G., Shao, B., Heinecke, J. W., and Oda, M. N. (2010) Exchange of apolipoprotein A-I between lipid-associated and lipid-free states: A potential target for oxidative generation of dysfunctional high density lipoproteins. *J. Biol. Chem. 285* (24), 18847−18857.

(10) Oram, J. F., and Heinecke, J. W. (2005) ATP-binding cassette transporter A1: A cell cholesterol exporter that protects against cardiovascular disease. *Physiol. Rev. 85* (4), 1343−1372.

(11) Mehta, R., Gantz, D. L., and Gursky, O. (2003) Human plasma high-density lipoproteins are stabilized by kinetic factors. *J. Mol. Biol. 328* (1), 183−192.

(12) Gursky, O., and Atkinson, D. (1996) Thermal unfolding of human high-density apolipoprotein A-1: Implications for a lipid-free molten globular state. *Proc. Natl. Acad. Sci. U.S.A. 93* (7), 2991−2995.

(13) Guha, M., Gao, X., Jayaraman, S., and Gursky, O. (2008) Structural stability and functional remodeling of high-density lipoproteins: The importance of being disordered. *Biochemistry 47* (44), 11393−11397.

(14) Lee, J. Y., Lanningham-Foster, L., Boudyguina, E. Y., Smith, T. L., Young, E. R., Colvin, P. L., Thomas, M. J., and Parks, J. S. (2004) Prebeta high density lipoprotein has two metabolic fates in human apolipoprotein A-I transgenic mice. *J. Lipid Res. 45* (4), 716−728.

(15) Ramella, N. A., Rimoldi, O. J., Prieto, E. D., Schinella, G. R., Sanchez, S. A., Jaureguiberry, M. S., Vela, M. E., Ferreira, S. T., and Tricerri, M. A. (2011) Human apolipoprotein A-I-derived amyloid: Its association with atherosclerosis. *PLoS One 6* (7), e22532.

(16) Teoh, C. L., Griffin, M. D., and Howlett, G. J. (2011) Apolipoproteins and amyloid fibril formation in atherosclerosis. *Protein Cell 2* (2), 116−127.

(17) Sorci-Thomas, M. G., and Thomas, M. J. (2002) The effects of altered apolipoprotein A-I structure on plasma HDL concentration. *Trends Cardiovasc. Med. 12* (3), 121−128.

(18) Obici, L., Franceschini, G., Calabresi, L., Giorgetti, S., Stoppini, M., Merlini, G., and Bellotti, V. (2006) Structure, function and amyloidogenic propensity of apolipoprotein A-I. *Amyloid 13* (4), 191−205.

(19) Gomaraschi, M., Obici, L., Simonelli, S., Gregorini, G., Negrinelli, A., Merlini, G., Franceschini, G., and Calabresi, L. (2011) Effect of the amyloidogenic L75P apolipoprotein A-I variant on HDL subpopulations. *Clin. Chim. Acta 412* (13−14), 1262−1265.

(20) Rowczenio, D., Dogan, A., Theis, J. D., Vrana, J. A., Lachmann, H. J., Wechalekar, A. D., Gilbertson, J. A., Hunt, T., Gibbs, S. D., Sattianayagam, P. T., Pinney, J. H., Hawkins, P. N., and Gillmore, J. D. (2011) Amyloidogenicity and clinical phenotype associated with five novel mutations in apolipoprotein A-I. *Am. J. Pathol. 179* (4), 1978−1987.

(21) Monti, D. M., Guglielmi, F., Monti, M., Cozzolino, F., Torrassa, S., Relini, A., Pucci, P., Arciello, A., and Piccoli, R. (2010) Effects of a lipid environment on the fibrillogenic pathway of the N-terminal polypeptide of human apolipoprotein A-I, responsible for in vivo amyloid fibril formation. *Eur. Biophys. J. 39* (9), 1289−1299.

(22) Gorbenko, G. P., and Kinnunen, P. K. (2006) The role of lipid-protein interactions in amyloid-type protein fibril formation. *Chem. Phys. Lipids 141* (1−2), 72−82.

(23) Rader, D. J., Gregg, R. E., Meng, M. S., Schaefer, J. R., Zech, L. A., Benson, M. D., and Brewer, H. B. Jr. (1992) In vivo metabolism of a mutant apolipoprotein, apoA-I Iowa, associated with hypoalphalipoproteinemia and hereditary systemic amyloidosis. *J. Lipid Res. 33* (5), 755−763.

(24) Marchesi, M., Parolini, C., Valetti, C., Mangione, P., Obici, L., Giorgetti, S., Raimondi, S., Donadei, S., Gregorini, G., Merlini, G., Stoppini, M., Chiesa, G., and Bellotti, V. (2011) The intracellular quality control system down-regulates the secretion of amyloidogenic apolipoprotein A-I variants: A possible impact on the natural history of the disease. *Biochim. Biophys. Acta 1812* (1), 87−93.

(25) de Sousa, M. M., Vital, C., Ostler, D., Fernandes, R., Pouget-Abadie, J., Carles, D., and Saraiva, M. J. (2000) Apolipoprotein AI and transthyretin as components of amyloid fibrils in a kindred with apoAI Leu178His amyloidosis. *Am. J. Pathol. 156* (6), 1911−1917.

(26) Obici, L., Bellotti, V., Mangione, P., Stoppini, M., Arbustini, E., Verga, L., Zorzoli, I., Anesi, E., Zanotti, G., Campana, C., Viganò, M., and Merlini, G. (1999) The new apolipoprotein A-I variant Leu(174) to Ser causes hereditary cardiac amyloidosis, and the amyloid fibrils are constituted by the 93-residue N-terminal polypeptide. *Am. J. Pathol. 155* (3), 695−702.

(27) Raimondi, S., Guglielmi, F., Giorgetti, S., Di Gaetano, S., Arciello, A., Monti, D. M., Relini, A., Nichino, D., Doglia, S. M., Natalello, A., Pucci, P., Mangione, P., Obici, L., Merlini, G., Stoppini, M., Robustelli, P., Tartaglia, G. G., Vendruscolo, M., Dobson, C. M., Piccoli, R., and Bellotti, V. (2011) Effects of the known pathogenic

mutations on the aggregation pathway of the amyloidogenic peptide of apolipoprotein A-I. *J. Mol. Biol. 407* (3), 465−476.
(28) Zhu, H. L., and Atkinson, D. (2007) Conformation and lipid binding of a C-terminal (198−243) peptide of human apolipoprotein A-I. *Biochemistry 46* (6), 1624−1634.
(29) Andreola, A., Bellotti, V., Giorgetti, S., Mangione, P., Obici, L., Stoppini, M., Torres, J., Monzani, E., Merlini, G., and Sunde, M. (2003) Conformational switching and fibrillogenesis in the amyloidogenic fragment of apolipoprotein A-I. *J. Biol. Chem. 278* (4), 2444−24451.
(30) McManus, D. C., Scott, B. R., Franklin, V., Sparks, D. L., and Marcel, Y. L. (2001) Proteolytic degradation and impaired secretion of an apolipoprotein A-I mutant associated with dominantly inherited hypoalphalipoproteinemia. *J. Biol. Chem. 276* (24), 21292−21302.
(31) Mei, X., and Atkinson, D. (2011) Crystal structure of C-terminal truncated apolipoprotein A-I reveals the assembly of HDL by dimerization. *J. Biol. Chem. 286* (44), 38570−38582.
(32) Borhani, D. W., Rogers, D. P., Engler, J. A., and Brouillette, C. G. (1997) Crystal structure of truncated human apolipoprotein A-I suggests a lipid-bound conformation. *Proc. Natl. Acad. Sci. U.S.A. 94* (23), 12291−12296.
(33) Chetty, P. S., Mayne, L., Lund-Katz, S., Stranz, D., Englander, S. W., and Phillips, M. C. (2009) Helical structure and stability in human apolipoprotein A-I by hydrogen exchange and mass spectrometry. *Proc. Natl. Acad. Sci. U.S.A. 106*, 19005−19010.
(34) Gomaraschi, M., Obici, L., Simonelli, S., Gregorini, G., Negrinelli, A., Merlini, G., Franceschini, G., and Calabresi, L. (2011) Effect of the amyloidogenic L75P apolipoprotein A-I variant on HDL subpopulations. *Clin. Chim. Acta 412* (13−14), 1262−1265.
(35) Jones, M. K., Gu, F., Catte, A., Li, L., and Segrest, J. P. (2011) "Sticky" and "promiscuous", the Yin and Yang of apolipoprotein A-I termini in discoidal high-density lipoproteins: A combined computational-experimental approach. *Biochemistry 50* (12), 2249−2263.
(36) Lagerstedt, J. O., Cavigiolio, G., Roberts, L. M., Hong, H. S., Jin, L. W., Fitzgerald, P. G., Oda, M. N., and Voss, J. C. (2007) Mapping the structural transition in an amyloidogenic apolipoprotein A-I. *Biochemistry 46* (34), 9693−9699.
(37) Jayaraman, S., Cavigiolio, G., and Gursky, O. (2012) Folded functional lipid-poor apolipoprotein A-I obtained by heating of high-density lipoproteins: Relevance to HDL biogenesis. *Biochem. J.*, DOI: doi: 10.1042/BJ20111831.
(38) Lagerstedt, J. O., Cavigiolio, G., Budamagunta, M. S., Pagani, I., Voss, J. C., and Oda, M. N. (2011) Structure of apolipoprotein A-I N terminus on nascent high density lipoproteins. *J. Biol. Chem. 286* (4), 2966−2975.
(39) Anantharamaiah, G. M., Hughes, T. A., Iqbal, M., Gawish, A., Neame, P. J., Medley, M. F., and Segrest, J. P. (1988) Effect of oxidation on the properties of apolipoproteins A-I and A-II. *J. Lipid Res. 29* (3), 309−318.
(40) Jonas, A., von Eckardstein, A., Churgay, L., Mantulin, W. W., and Assmann, G. (1993) Structural and functional properties of natural and chemical variants of apolipoprotein A-I. *Biochim. Biophys. Acta 1166* (2−3), 202−210.
(41) Sigalov, A. B., and Stern, L. J. (2001) Oxidation of methionine residues affects the structure and stability of apolipoprotein A-I in reconstituted high density lipoprotein particles. *Chem. Phys. Lipids 113* (1−2), 133−146.
(42) Hatters, D. M., and Howlett, G. J. (2002) The structural basis for amyloid formation by plasma apolipoproteins: A review. *Eur. Biophys. J. 31* (1), 2−8.
(43) Wong, Y. Q., Binger, K. J., Howlett, G. J., and Griffin, M. D. (2010) Methionine oxidation induces amyloid fibril formation by full-length apolipoprotein A-I. *Proc. Natl. Acad. Sci. U.S.A. 107* (5), 1977−1982.
(44) Jayaraman, S., Gantz, D. L., and Gursky, O. (2011) Effects of phospholipase A_2 and its products on structural stability of human LDL: Relevance to formation of LDL-derived lipid droplets. *J. Lipid Res. 52* (3), 549−557.
(45) Sparks, D. L., Davidson, W. S., Lund-Katz, S., and Phillips, M. C. (1995) Effects of the neutral lipid content of high density lipoprotein on apolipoprotein A-I structure and particle stability. *J. Biol. Chem. 270* (45), 26910−26917.